JOURNAL OF VIROLOGY, Feb. 2011, p. 1777–1792 Vol. 85, No. 4
0022-538X/11/$12.00 doi:10.1128/JVI.02170-10

Identification of New Functional Regions in Hepatitis C Virus Envelope Glycoprotein E2[▽]

Anna Albecka,[1] Roland Montserret,[2] Thomas Krey,[3] Alexander W. Tarr,[4] Eric Diesis,[2] Jonathan K. Ball,[4] Véronique Descamps,[5] Gilles Duverlie,[5] Felix Rey,[3] François Penin,[2]# and Jean Dubuisson[1]*#

Institut Pasteur de Lille, Center for Infection and Immunity of Lille (CIIL), F-59019 Lille, France; Inserm U1019, F-59019 Lille, France; CNRS UMR8204, F-59021 Lille, France; and Université Lille Nord de France, F-59000 Lille, France[1]; Institut de Biologie et Chimie des Protéines, UMR-5086-CNRS, Université de Lyon, Lyon, France[2]; Institut Pasteur, CNRS URA3015, Unité de Virologie Structurale, Paris, France[3]; School of Molecular Medical Sciences, the University of Nottingham, Queen's Medical Centre, Nottingham, United Kingdom[4]; and Laboratoire de Virologie EA4294, Centre Hospitalier Universitaire d'Amiens, Université de Picardie Jules Verne, Amiens, France[5]

Received 15 October 2010/Accepted 29 November 2010

Little is known about the structure of the envelope glycoproteins of hepatitis C virus (HCV). To identify new regions essential for the function of these glycoproteins, we generated HCV pseudoparticles (HCVpp) containing HCV envelope glycoproteins, E1 and E2, from different genotypes in order to detect intergenotypic incompatibilities between these two proteins. Several genotype combinations were nonfunctional for HCV entry. Of interest, a combination of E1 from genotype 2a and E2 from genotype 1a was nonfunctional in the HCVpp system. We therefore used this nonfunctional complex and the recently described structural model of E2 to identify new functional regions in E2 by exchanging protein regions between these two genotypes. The functionality of these chimeric envelope proteins in the HCVpp system and/or the cell-cultured infectious virus (HCVcc) was analyzed. We showed that the intergenotypic variable region (IgVR), hypervariable region 2 (HVR2), and another segment in domain II play a role in E1E2 assembly. We also demonstrated intradomain interactions within domain I. Importantly, we also identified a segment (amino acids [aa] 705 to 715 [segment 705-715]) in the stem region of E2, which is essential for HCVcc entry. Circular dichroism and nuclear magnetic resonance structural analyses of the synthetic peptide E2-SC containing this segment revealed the presence of a central amphipathic helix, which likely folds upon membrane binding. Due to its location in the stem region, segment 705-715 is likely involved in the reorganization of the glycoprotein complexes taking place during the fusion process. In conclusion, our study highlights new functional and structural regions in HCV envelope glycoprotein E2.

Hepatitis C virus (HCV) infects approximately 3% of the world population (72) and is currently the major cause of chronic hepatitis, cirrhosis, and hepatocellular carcinoma (43). A vaccine is not yet available, and the treatment fails in around 50% of the cases, depending on the virus genotype (43). Although the cloning of the HCV genome more than 20 years ago (4) allowed for a rapid analysis of the genomic organization and a biochemical characterization of its proteins (reviewed in reference 57), the lack of a cell culture system to efficiently amplify this virus has long been a major obstacle for the study of the HCV life cycle. Fortunately, in 2005, the development of a cell culture system that allowed for a relatively efficient amplification of HCV (HCVcc) was finally reported (42, 71, 78).

HCV is an enveloped, positive-stranded RNA virus that belongs to the *Flaviviridae* family (41). Its genome encodes a single polyprotein of about 3,000 amino acids, which is cleaved co- and posttranslationally by cellular and viral proteases to yield at least 10 mature products (reviewed in reference 57). Cleavage of the viral polyprotein by a cellular signal peptidase gives rise to the envelope glycoproteins E1 and E2 (reviewed in reference 17). HCV envelope glycoproteins are type I transmembrane (TM) proteins containing a highly glycosylated N-terminal ectodomain (28) and a C-terminal TM domain (8). During their synthesis, E1 and E2 ectodomains are translocated inside the lumen of the endoplasmic reticulum (ER), and their TM domains are inserted in the membrane of this compartment (8). During their biogenesis, E1 and E2 assemble as noncovalent heterodimers, which are retained in the ER (11). Interestingly, the TM domains of HCV envelope glycoproteins have been shown to contain determinants of E1E2 interactions (53).

The development of retroviral pseudotypes containing HCV glycoproteins (HCVpp) has been the first tool available to study the role of HCV envelope proteins in virus entry (1, 14, 29). HCV glycoprotein heterodimers are involved in interaction(s) with a cellular receptor(s) (54) and mediate fusion with cellular membranes (27, 39, 40, 63). The tetraspanin CD81, the scavenger receptor BI (SR-BI), and the tight junction proteins claudin 1 and occludin have all been identified as essential for entry (reviewed in reference 61), but direct binding of the E1E2 heterodimer has been confirmed only for CD81 (7, 60).

* Corresponding author. Mailing address: Molecular and Cellular Virology of Hepatitis C, CIIL, Inserm (U1019) and CNRS (UMR8204), Institut Pasteur de Lille, Bâtiment IBL, 1 rue Calmette, BP447, 59021 Lille cedex, France. Phone: (33) 3 20 87 11 60. Fax: (33) 3 20 87 12 01. E-mail: jean.dubuisson@ibl.fr.

J.D. and F.P. are equal senior coauthors of this work.

▽ Published ahead of print on 8 December 2010.

The secondary and tertiary structures of glycoproteins are supposed to be similar among the members of the *Flaviviridae* family, suggesting that HCV envelope glycoproteins should belong to class II fusion proteins (reviewed in reference 32). In this model, the fusion protein is located downstream on the polyprotein encoded by the virus, and the companion protein located immediately upstream is a chaperone involved in the folding of the fusion protein. These observations as well as the identification of E2 disulfide bonds led to a model of the E2 ectodomain, consisting of three separate domains (34). Domain I (DI) consists of eight β strands and is extended on the N terminus by hypervariable region 1 (HVR1). This domain contains determinants for CD81 interaction. Domain II (DII) includes hypervariable region 2 (HVR2), and its most conserved part is suggested to act as a fusion loop (amino acids [aa] 502 to 520). DI is connected to domain III (DIII) by a linker region called the intergenotypic variable region (IgVR). Finally, DIII is connected to the TM domain by the flexible stem (ST) region. This model characterizes E2 as a complex structure in which intramolecular interactions as well as the association with E1 glycoprotein are required for receptor interactions and membrane fusion.

HCV can be grouped into seven genotypes (24), but the overall structure and functions of the E1E2 heterodimer do not differ significantly between HCV genotypes. However, due to their cooperative interaction (38), HCV envelope glycoproteins have likely coevolved in the different genotypes, and this coevolution may lead to functional intergenotypic incompatibilities between E1 and E2. We therefore generated HCVpp containing HCV envelope glycoproteins from different genotypes to test the intergenotypic incompatibilities between these two proteins. We showed that several combinations of E1 and E2 from different genotypes were nonfunctional for HCV entry. We then used the HCVpp and HCVcc systems to map functional regions in HCV glycoprotein E2. This led to the identification of several regions of the E2 ectodomain that play a role in E1E2 assembly as well as a ST segment, which is involved in HCVcc entry. To better understand the role of the latter segment, an additional structural characterization of the C-terminal part of the ST was performed. Circular dichroism (CD) and nuclear magnetic resonance (NMR) analyses of a synthetic peptide denoted E2-SC revealed the presence of an amphipathic helix exhibiting lipid-binding properties. This helix is expected to fold upon membrane binding, but its limited stability suggests that it could easily switch from helical to random conformation, depending on its microenvironment and/or binding partners. Together, these data reveal new structure-function relationships for HCV envelope glycoprotein E2.

MATERIALS AND METHODS

Cell culture. HEK293T human embryo kidney cells and Huh-7 human hepatoma cells (52) were grown in Dulbecco's modified essential medium (Invitrogen) supplemented with 10% fetal bovine serum.

Antibodies. Monoclonal antibodies (MAbs) A4 (anti-E1) (16), 3/11 (anti-E2; kindly provided by J. A. McKeating, University of Birmingham, United Kingdom) (20), and anti-murine leukemia virus capsid (MAb R187; ATCC CRL1912) were produced *in vitro* using a MiniPerm apparatus (Heraeus) as recommended by the manufacturer.

Plasmids and mutagenesis. DNA sequences used in the studies were based on genotype 2a (JFH-1; GenBank accession number AB237837), 1a (UKN1A-14.42; accession number AY734972), 1b (UKN1B-5.23; accession number AY734976), 2b (UKN2B-1.1; accession number AY734982), and 1a (H77 strain; accession number AAB67037, with three amino acid changes at the following positions: R564C, V566A, and G650E). Sequences of E1 and E2 glycoproteins with their signal sequence were cloned together as a polyprotein or separately into the pcDNA3.1+ vector. To obtain chimeric constructs, full-length or fragments of glycoprotein E2 from isolate JFH-1 were replaced by the corresponding regions from isolate H77. These plasmids were constructed by two-step PCR using Native *Pfu* DNA polymerase (Stratagene). All of the constructs were sequenced and verified by CLUSTAL W software.

HCVpp assay. 293T cells were transfected with plasmids murine leukemia virus (MLV) Gag-Pol, MLV-luc, and pcDNA3.1+E1E2 as described previously (54). For some of the experiments, E1 and E2 were expressed from two separate vectors, pcDNA3.1+E1 and pcDNA3.1+E2. Plasmid pcDNA3.1+ containing no envelope protein gene was used as a negative control. After 48 h, supernatants containing pseudoparticles were filtered through a 0.45-μm-pore-size membrane and used to infect Huh-7 cells or pelleted by ultracentrifugation through a 20% sucrose cushion and analyzed by Western blotting. 293T cells were lysed with 1% Triton X-100 and analyzed by Western blotting. Infectivity of HCVpp on target Huh-7 cells was assessed after 48 h by using a firefly luciferase reporter gene activity kit (Promega), as recommended by the manufacturer. Results are presented as the means ± standard deviations of results of three independent experiments. Graphs were made using Prism software.

CD81 pull-down assay. Recombinant fusion proteins containing the large extracellular loop of CD81 fused to glutathione *S*-transferase (GST) were preadsorbed onto glutathione-Sepharose beads (Pharmacia Biotech) and then incubated with lysates of pseudoparticle-producing cells. After overnight incubation, beads were extensively washed with lysis buffer. Pull down was followed by Western blotting to detect E1 and E2.

Western blotting. After separation by sodium dodecyl sulfate (SDS)-PAGE, proteins were transferred to nitrocellulose membranes (Hybond-ECL; Amersham) by using a Trans-Blot apparatus (Bio-Rad) and revealed with specific antibodies (anti-E1 and anti-E2) followed by secondary immunoglobulin conjugated to peroxidase. The proteins of interest were revealed by enhanced chemiluminescence detection (ECL; Amersham) as recommended by the manufacturer.

HCVcc assay. Viral RNA of isolate JFH-1 containing the *Renilla* luciferase gene, A4 epitope, and cysteine and serine (CS) mutations in the capsid was prepared as described previously (12, 25). A replication-deficient clone containing a GND mutation in the NS5B active site and the assembly-deficient ΔE1E2 clone (71) were used as negative controls. Huh-7 cells (2×10^6) were mixed with 25 μg of RNA, placed in 0.2-cm cuvette (Bio-Rad), and electroporated with one pulse at 1,000 μF and 150 V using a GenePulser Xcell electroporator (Bio-Rad). After 10 min, cells were mixed with fresh medium and seeded into tissue culture dishes. After 4 h, a portion of the electroporated cells was lysed to verify the translation from the electroporated RNA for the different chimeras. Replication was tested after 24, 48, and 72 h posttransfection. Supernatants were collected after 72 h, centrifuged to remove cell debris, and used to infect Huh-7 cells. To assess intracellular infectivity, cells were washed with phosphate-buffered saline (PBS), trypsinized, and pelleted. Pellets were resuspended in medium and lysed by three freeze-thaw cycles. Cell lysates were clarified by centrifugation at $10{,}000 \times g$ for 5 min. Supernatants containing extracellular and intracellular virus were incubated with the cells for 2 h. Infectivity of the produced viral chimeras was verified after 48 h by using a *Renilla* luciferase activity kit (Promega), as indicated by the manufacturer. Results are presented as the means ± standard deviations of results of three independent experiments. Graphs were made using Prism software.

HCV core quantification assay. HCVcc supernatants were collected 72 h after electroporations. The core was quantified by an automated chemiluminescent microparticle immunoassay according to the instructions of the manufacturer (Architect HCVAg, Abbott, Germany) (47, 51).

Sequence analyses and predictions. Sequence analyses were performed using tools available at the Institut de Biologie et Chimie des Protéines (IBCP), i.e., by using the Network Protein Sequence Analysis (NPSA) website (http://npsa-pbil.ibcp.fr) (9). Provisional and confirmed genotyped HCV E2 sequences were retrieved from the European HCV database (http://euhcvdb.ibcp.fr/) (10). Multiple-sequence alignments were performed with CLUSTAL W (69), using the default options. The repertoire of residues at each amino acid position and their frequencies observed for natural sequence variants were computed by the use of a program developed at the IBCP (F. Dorkeld, C. Combet, F. Penin, and G.

Deleage, unpublished data). Protein secondary structures were deduced from a large set of prediction methods available at the NPSA website, including HNNC, SIMPA96, MLRC, SOPM, PHD, and Predator (see http://npsa-pbil.ibcp.fr/NPSA and the references therein). Interfacial hydrophobicity plots were generated with MPEx (http://blanco.biomol.uci.edu/mpex/) by using the scale developed by Wimley and White (74).

Peptide synthesis and purification. The E2-SC peptide, representing amino acids 684 to 719 of E2 from the HCV strain JFH-1 (accession number AB047639; SDLPALSTGLLHLHQNIVDVQYMYGLSPAITKYVVR), was synthesized in in-house facilities and purified by reverse-phase high-pressure liquid chromatography (HPLC) on a Nucleosil C_{18} column (120 Å, 5 μm) using a water/acetonitrile gradient containing 0.1% trifluoroacetic acid. The peptide was eluted as a single peak at 44% acetonitrile. The peak was identified by mass spectroscopy as the expected molecular mass peptide (observed molecular weight [MW + H^+], 4,013.35; calculated molecular mass, 4,013.68 Da).

CD. Far-UV circular dichroism (CD) spectra were recorded with a Chirascan spectrometer (Applied Photophysics, United Kingdom) calibrated with 1S-(+)-10-camphorsulfonic acid. Measurements were carried out at 25°C in a 0.1-cm-path-length quartz cuvette (Hellma), with a typical peptide concentration of 20 μM. Spectra were measured in a 180-nm to 260-nm wavelength range with a increment of 0.2 nm, band pass of 0.5 nm, and integration time of 1 s. Spectra were processed, baseline corrected, smoothed, and converted with Chirascan software. Spectral units were expressed as the mean molar ellipticity per residue by using the peptide concentration determined with UV light absorbance directly measured with a CD cell at 280 nm (e = 3,900 M^{-1} cm^{-1}) of the peptide solubilized in a solution of 50% 2,2,2-trifluoroethanol (TFE) in water. Estimation of the secondary structure content was carried out using the DICHROWEB server facilities (http://dichroweb.cryst.bbk.ac.uk/) (73).

NMR spectroscopy. The purified peptide E2-SC was dissolved in either 100 mM deuterated SDS (SDS-d_{25}) or 50% deuterated TFE (TFE-d_2; 99%) in H_2O (vol/vol), and 2,2-dimethyl-2-silapentane-5-sulfonate was added to the NMR samples as an internal ^{1}H chemical shift reference. Multidimensional experiments were performed at 25°C with a Bruker Avance 500 MHz spectrometer using standard homonuclear pulse sequences, including nuclear Overhauser enhancement spectroscopy (NOESY) (mixing times, between 100 and 150 ms) and clean total correlation spectroscopy (TOCSY) (isotropic mixing time of 85 ms), as detailed previously (18, 58). Water suppression was achieved by presaturation. Bruker Topspin software was used to process all data, and Sparky was used for spectral analysis (http://www.cgl.ucsf.edu/home/sparky/). Intraresidue backbone resonances and aliphatic side chains were identified from homonuclear ^{1}H TOCSY experiments and confirmed with ^{1}H-^{13}C heteronuclear single-quantum correlation (HSQC) experiments in ^{13}C natural abundance. Sequential assignments were determined by correlating intraresidue assignments with interresidue cross peaks observed in bidimensional ^{1}H NOESY. NMR-derived ^{1}Hα and ^{13}Cα chemical shifts were reported relative to the random coil chemical shifts in SDS (65) and TFE (48), respectively.

NMR-derived constraints and structure calculation. Nuclear Overhauser enhancement (NOE) intensities used as input for structure calculations were obtained from the NOESY spectrum recorded with a 150-ms mixing time and checked for spin diffusion on spectra recorded at lower mixing times (100 ms). NOEs were partitioned into three categories of intensities that were converted into distances ranging from a common lower limit of 1.8 Å to upper limits of 2.8 Å, 3.9 Å, and 5.0 Å, respectively. Protons without stereospecific assignments were treated as pseudoatoms, and the correction factors were added to the upper distance constraints (76). Neither hydrogen bond nor dihedral angle constraints were introduced. Three-dimensional structures were generated from NOE distances with the standard torsion angle molecular dynamics protocol in the XPLOR-NIH 2.24 program (66) using the standard force fields and default parameter sets. A set of 50 structures was initially calculated to widely sample the conformational space, and the structures of low energy with neither distance nor dihedral angle restraint violations were retained. The selected structures were compared by pairwise root mean square deviation (RMSD) over the backbone atom coordinates (N, Cα, and C′). Statistical analyses, superimpositions of structures, and structural analyses were performed with MOLMOL (33), and the quality of the selected structures was checked with the Research Collaboratory for Structural Bioinformatics (RCSB) Protein Data Bank (PDB) validation server.

Accession numbers. The atomic coordinates for the NMR structure of peptide E2-SC and the NMR restraints in 50% TFE are available in the RCSB PDB under accession number 2KZQ (RCSB identification code 101755). The chemical shifts of all E2-SC residues have been deposited in BioMagResBank (BMRB) under accession number 17011.

RESULTS

HCVpp containing E1 and E2 from different genotypes identify genetic incompatibilities between some HCV genotypes. HCV is currently classified into seven genotypes and several subtypes that at the nucleotide level differ from each other by 31 to 33% and 20 to 25%, respectively (36, 67). To test the intergenotypic incompatibilities between E1 and E2, we selected a limited number of E1E2 sequences from different genotypes/subtypes (1a, 1b, 2a, and 2b). We constructed a series of plasmids expressing E1 alone or E2 alone, so we could easily coexpress E1 and E2 in *trans* from different genotypes/subtypes to produce HCVpp. However, since we did not have access to an anti-E1 antibody that recognizes all these genotypes, we mutated a few residues in E1 to generate the A4 epitope at the N terminus of the protein (16) to facilitate the detection of this protein in our experiments (Fig. 1C). This epitope is present in some HCV isolates of genotype 1a, and such a modification in the context of HCVcc does not alter infectivity (25). We confirmed that this mutation allows for the detection of E1 (Fig. 1E), and we showed that it had only a moderate effect on HCVpp infectivity. Indeed, the infectivity of A4 epitope-containing pseudoparticles was reduced to 24% and 33% of the wild-type HCVpp levels for JFH-1 and the genotype 2b isolate (data not shown), respectively, whereas an increase in HCVpp infectivity to 220% was observed for the genotype 1b isolate (data not shown). Since all the constructs tested remained infectious, the mutant E1 proteins could be used to test the intergenotypic incompatibilities between E1 and E2. For the detection of E2, we used the 3/11 MAb (20), which recognizes a conserved minimum epitope (29).

We then tested the intergenotypic incompatibilities between E1 and E2 by producing HCVpp containing different combinations of envelope glycoproteins and assessed their infectivity. The intergenotypic combinations were compared to HCVpp produced with E1E2 from the reference genotypes/subtypes. HCVpp infectivity was reduced to background levels for some combinations, whereas it was moderately affected for others (data not shown). Surprisingly, chimeras with glycoprotein E1 from genotype 1a always showed an increase in infectivity compared to the reference genotypes, which was not the case for E1 from other genotypes. To test whether this phenomenon is specific for E1 from the H77 strain or if it is a more general feature of genotype 1a isolates, we analyzed the phenotype induced by the presence of E1 from another genotype 1a isolate (the UKN1a.14.42 isolate). Only when coexpressed with E2 from genotype 2b did the UKN1a.14.42 isolate induce an increase in HCVpp infectivity, whereas the other combinations remained as infectious as the control HCVpp containing E1E2 proteins from the UKN1a.14.42 isolate (data not shown). These data indicate that E1 from genotype 1a is functionally compatible with E2 from different genotypes/subtypes. Furthermore, it can also potentially increase the entry efficiency of HCVpp in some combinations. Although this phenotype is potentially interesting to explore, it was beyond the scope of this work. We were indeed interested by combinations of E1 and E2 inducing a defect in infectivity. Importantly, our results showed that several combinations abolish HCVpp infectivity, indicating structural incompatibilities between some genotypes or subtypes.

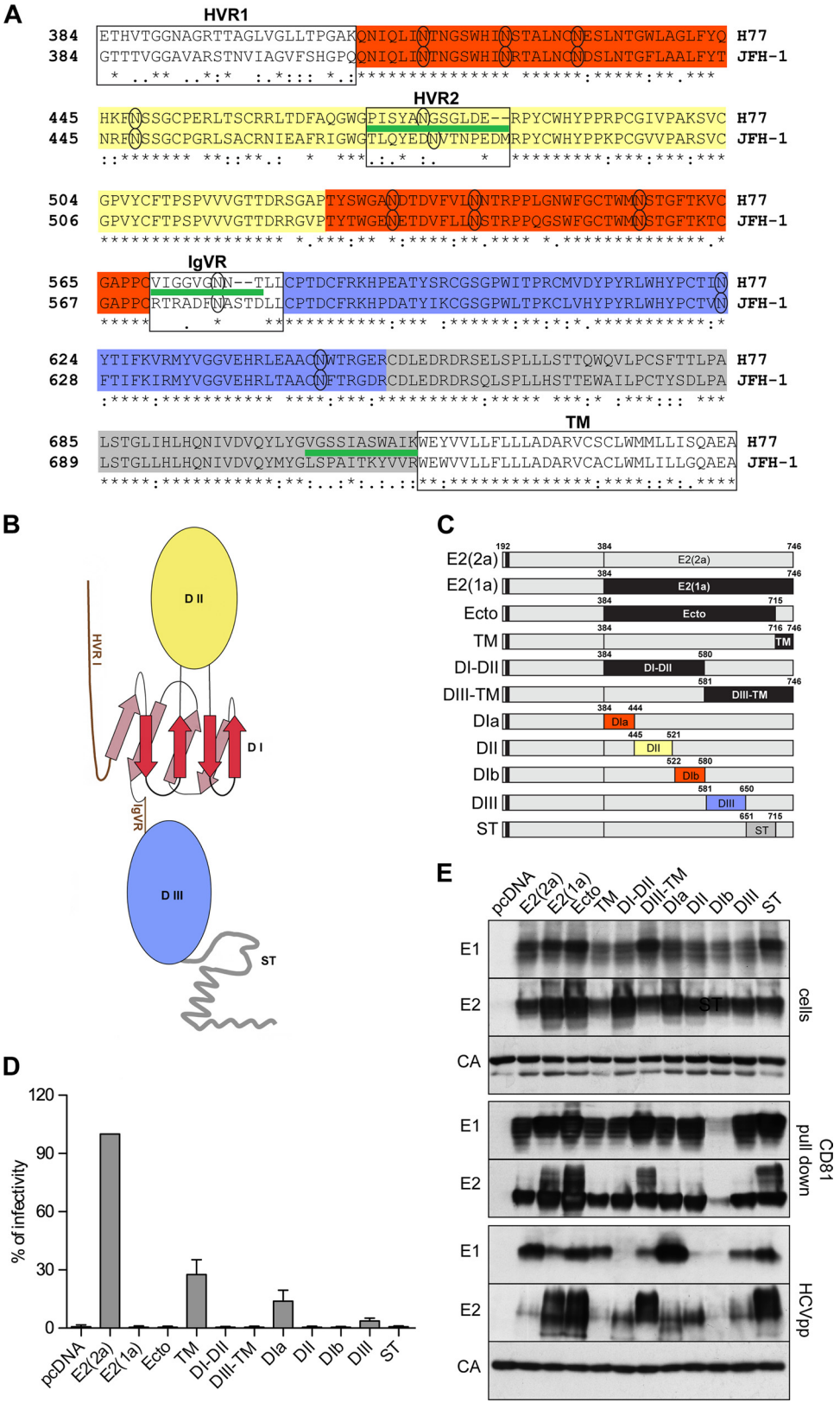

FIG. 1. Identification of regions within E2 responsible for intergenotypic incompatibilities. (A) Protein alignment of E2 glycoprotein from genotypes 1a (H77) and 2a (JFH-1). Previously characterized regions, such as HVR1, HVR2, IgVR, and TM, are marked with rectangles. Colors correspond to the E2 domains: DI in red, DII in yellow, DIII in blue, and ST in gray (34). Glycosylation sites are circled. Determinants of intergenotypic incompatibilities are underlined in green. Alignment was performed with CLUSTAL W software. (B) Hypothetical structural model of E2 glycoprotein (34). Colors of the domains correspond to the protein regions of the alignment presented in panel A. (C) Schematic

Several E2 regions are responsible for intergenotypic incompatibility. Although our first screening for nonfunctional chimeras indicated that several combinations lead to nonfunctional HCVpp, for a more in-depth analysis, we decided to focus on a single chimera for the identification of E2 determinants of intergenotypic incompatibility. We selected the combination containing E1 sequence from genotype 2a (JFH-1 isolate) and E2 from genotype 1a (H77 isolate). It should be noted that the A4 epitope was also reconstructed in this E1 sequence to facilitate its detection by Western blotting. In addition, derived constructs of this combination could easily be transferred into the HCVcc system (see below). Furthermore, we expressed E1 and E2 proteins from the same polyprotein to have both proteins expressed in *cis* instead of in *trans*. Under these conditions, we can be sure that the same amounts of E1 and E2 are coexpressed in cells producing HCVpp. Furthermore, this type of expression better mimics the polyprotein processing observed in the context of HCV infection.

To identify the E2 determinant(s) responsible for incompatibility between E1(2a) and E2(1a), we constructed a series of chimeras in the context of E1E2 of genotype 2a in which E2 regions were replaced by the corresponding sequence from genotype 1a (Fig. 1C), and their infectivity was analyzed in the context of the HCVpp system (Fig. 1D). These constructs were designed based on the recently proposed model of E2 (Fig. 1A and B) (34). HCVpp containing E1(2a)E2(2a) and E1(2a)E2(1a) was used as a positive and negative control, respectively. As shown in Fig. 1D, HCVpp was no longer infectious when E2(1a) ectodomain (Ecto) was introduced in the context of E1E2 of genotype 2a, whereas replacement of the TM domain only moderately reduced HCVpp infectivity, suggesting that the major determinant(s) leading to functional incompatibilities is located in the ectodomain of E2. Furthermore, when the DI-DII region or DIII-TM region of genotype 1a was introduced in the context of E1E2 of genotype 2a, HCVpp was also no longer infectious, indicating that at least two regions in the ectodomain of E2 contain determinants leading to intergenotypic incompatibility. Finally, analyses of chimeras DIa, DII, DIb, DIII, and ST indicated that regions responsible for intergenotypic incompatibilities are located in DII, DIb, and ST. The DIa construct was still moderately infectious, and DIII showed some residual infectivity. Even if they reduce HCVpp entry, these two regions do not contain genotype-specific determinants that are essential for HCV entry in the HCVpp system.

HCVpp generated with these chimeric proteins was also characterized for the presence of viral proteins and compared to cell lysates expressing these proteins. As shown in Fig. 1E, the levels of expression of MLV capsid, E1, and E2 were similar in cell lysates for all the constructs. However, the signals for E1 and E2 varied in some constructs in the context of HCVpp. Some of the variations in the intensity of E2 can be explained partly by differences in affinities of the MAb for its epitope in the context of the different genotypes as previously shown (46, 68). Indeed, when E2 or its ectodomain were from genotype 1a, the intensity of the signal was higher in HCVpp. A higher signal for E2 was also observed for the constructs containing the ST region of genotype 1a (Fig. 1E, DIII-TM and ST), suggesting that the ST region might modulate the recognition of the 3/11 epitope. Due to the distance between the 3/11 epitope (located in DI) and the ST region, this might be due to an indirect effect of the ST region. One possibility is that in the context of E1E2 of genotype 2a, the ST region of genotype 1a indirectly affects the processing of the glycans as suggested by a difference in the migration pattern similar to what has been observed by others when mutations are introduced in E1 (63). Glycan processing can in turn modulate the binding of MAb 3/11 as suggested for other anti-E2 MAbs (19). It is important to note that the level of incorporation of E2 into HCVpp does not reflect the level of infectivity. Indeed, mutant TM was the most infectious chimera; however, the level of incorporation of E2 appeared rather low for this virus. In the case of E1, the protein is from the same genotype, so the differences in the level of incorporation into HCVpp directly reflect the effect of the change induced by the chimeric E2 constructs. It is worth noting that the level of E1 was close to background for DI-DII, DII, and DIb constructs. The absence of infectivity of these constructs might therefore be due to the lack of incorporation of E1 into HCVpp. Surprisingly, in the case of DIa, a higher level of incorporation of E1 was observed. However, this was not correlated with a higher level of incorporation of E2 into HCVpp.

Finally, we also analyzed the recognition of intracellular E1E2 complexes by CD81. As shown in Fig. 1E, E1 and E2 obtained from cell lysates were precipitated with the CD81 large extracellular loop (CD81LEL) for all the constructs except DIb. These data indicate that, except for DIb, exchanging E2 regions between 1a and 2a genotypes does not dramatically affect E2 folding or its potential to interact with E1 or CD81.

representation of chimeric E1E2 constructs used in the study. All chimeras contain E1 from genotype 2a and E2 from genotype 2a in which corresponding regions from genotype 1a have been introduced. The numbers correspond to the first and the last residue of the exchanged regions based on the numbering of the reference strain H77. Fragments from genotype 2a are shown in light gray. Fragments from genotype 1a are marked in black or in the color corresponding to specific E2 domains. The DI construct includes DI and HVR1. DIa′ includes HVR1 and segment 412-444 from DI. The DIb construct includes segment 522-569 from DI and IgVR. Note that the N terminus of E1 has been modified to reconstruct the A4 epitope present in E1 of genotype 1a, as indicated by a black box at the N terminus of E1. For this purpose, amino acid sequence TSSSYMVTNDC at position 197 to 207 of E1 of genotype 2a has been modified to SSGLYHVTNDC (modified amino acids are underlined). (D) Infectivity of chimeric HCVpp. Huh-7 cells were infected with chimeric pseudoparticles. The infectivity levels were assessed by the activity of the reporter luciferase gene. The results are presented as the percentage of infectivity in comparison to wild-type 2a HCVpp. The noninfectious particles containing no envelope proteins (pcDNA) were used as a negative control. (E) Western blotting of chimeric HCVpp. Cells producing HCVpp were lysed and analyzed by Western blotting. HCVpp were concentrated on a 20% sucrose cushion and analyzed by Western blotting. E1E2 was pulled down from the cell lysates by a CD81LEL-GST assay. E1, E2, and capsid were detected using MAbs A4, 3/11, and R187, respectively.

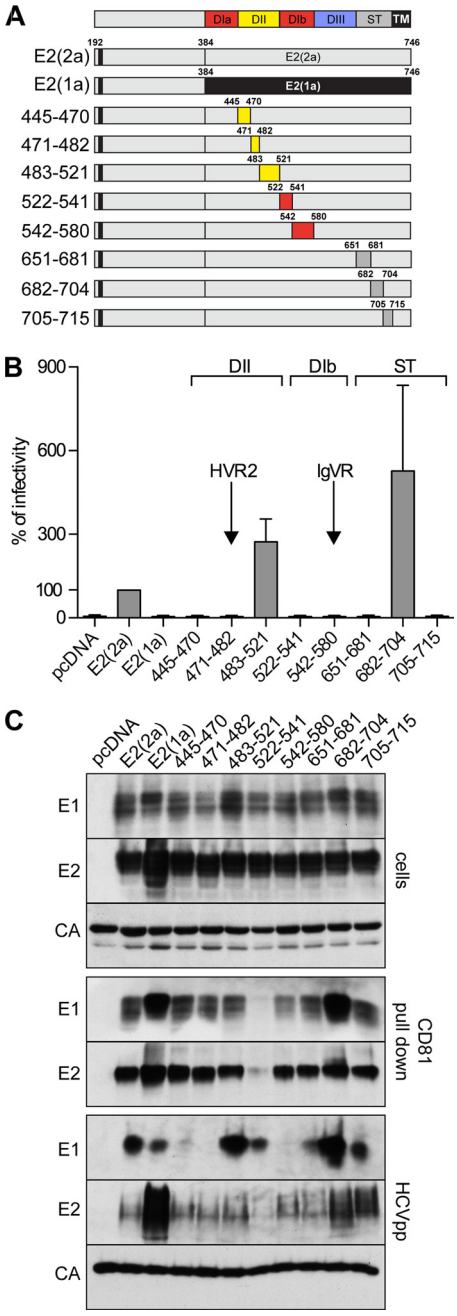

FIG. 2. Identification of E2 determinants of intergenotypic incompatibility. (A) Schematic representation of chimeric E1E2 constructs used in the study. All chimeras contain E1 from genotype 2a and E2 from genotype 2a in which corresponding regions from genotype 1a have been introduced. The numbers correspond to the first and last residues of the exchanged regions based on the numbering of the reference strain H77. Fragments from genotype 2a are shown in light gray. Fragments from genotype 1a are shown in black or in the color corresponding to specific E2 domains. As shown in Fig. 1C, the N terminus of E1 has been modified to reconstruct the A4 epitope present in E1 of genotype 1a as indicated by a black box at the N terminus of E1. (B) Infectivity of chimeric HCVpp with exchanged regions within DII (aa 445-470, 471-482, 483-521), DIb (aa 522-541, 542-580), and ST (aa 651-681, 682-704, 705-715). HCVpp infectivity was determined by measuring the activity of the luciferase reporter gene. Segment 471-482 corresponds to HVR2, and segment 542-580 includes part of DIb and IgVR. (C) Western blotting of chimeric HCVpp. Cells producing HCVpp were lysed and analyzed by Western blotting. HCVpp was concentrated on a 20% sucrose cushion and analyzed by Western blotting. E1E2 was pulled down from the cell lysates by a CD81LEL-GST assay. E1, E2, and capsid were detected using MAbs A4, 3/11, and R187, respectively.

Furthermore, the lack of infectivity of DIb is likely due to protein misfolding as shown in the CD81 pull-down.

Altogether, our data indicate that three regions (DII, DIb, and ST) contain determinants responsible for intergenotypic incompatibility. Furthermore, the lack of incorporation of E1 into HCVpp of DII and DIb chimeras suggests a defect in HCVpp assembly for these two constructs.

Identification of E2 determinants of intergenotypic incompatibility. To identify more precisely the E2 determinants of intergenotypic incompatibility, an additional series of chimeras was produced, which contained smaller segments of E2 of genotype 1a in the context of E1E2 of genotype 2a containing the A4 epitope (Fig. 2A). As shown in Fig. 2B and summarized in Table 1, changing the segment of aa 445 to 470 (segment 445-470) or 471-482 (HVR2) in DII, segment 522-541 or 542-580 (IgVR) in DIb, and segment 651-681 or 705-715 in the ST region abolished HCVpp infectivity. In contrast, changing segment 483-521 or 682-704 did not abolish HCVpp infectivity; inversely, it led to some increase in HCV entry.

HCVpp generated with these chimeric proteins were also characterized for the presence of viral proteins, and these results were compared to those for cell lysates expressing these proteins. As shown in Fig. 2C, the levels of expression of MLV capsid, E1, and E2 were similar in cell lysates for all the constructs. However, the signals for E1 and E2 varied in some constructs in the context of HCVpp. As discussed above, some variations were observed for E2, which might be due in part to differences in affinity of the 3/11 antibody for the E2 chimeras. In the case of E1, the level of incorporation into HCVpp directly reflects the effect of the change induced by the chimeric E2 constructs. It is worth noting that the level of E1 was close to background for 445-470, 471-482, and 542-580 constructs. The absence of infectivity of these constructs might therefore be due to the lack of incorporation of E1 into HCVpp. Furthermore, there was a lower level of incorporation of E1 and E2 for the 522-541 construct.

Finally, we also analyzed the recognition of intracellular E1E2 complexes by CD81. As shown in Fig. 2C, E1 and E2 obtained from cell lysates were precipitated with CD81LEL for all the constructs except 522-541. These data indicate that, except for the 522-541 segment, exchanging E2 regions between 1a and 2a genotypes does not dramatically affect E2 folding or its potential to interact with E1 or CD81. Furthermore, the lack of infectivity of the 522-541 construct is likely due to protein misfolding as shown in the CD81 pull-down.

Altogether, our data indicate that E2 contains six determinants responsible for intergenotypic incompatibility (445-470, 471-482, 522-541, 542-580, 651-681, and 705-715) (Fig. 2B). Furthermore, the lack of incorporation of E1 into HCVpp of 445-470, 471-482, and 542-580 chimeras as well as the reduced levels of E1E2 for the 522-541 chimera suggest a defect in HCVpp assembly for these four determinants (Fig. 2C). Finally, the lack of infectivity of chimeras 651-681 and 705-715

TABLE 1. Summary of the properties of E2 determinants tested in the HCVpp and/or HCVcc systems and their potential function in HCV assembly or entry

Domain	Region	HCVpp[a] infectivity	HCVcc[b]		Function
			Infectivity	Secretion	
Domain I	DIa 384-444	+	ND	ND	Both required for DI folding
	DIb 522-541	−	ND	ND	Both required for DI folding
Domain II	445-470	−	+	−	Assembly
	471-482 (HVR2)	−	−	−	Assembly
	483-521	+++	ND	ND	
IgVR	570-578	−	−	−	Assembly
Domain III	581-650	±	ND	ND	
Stem	651-681	−	+	+	
	682-704	+++	++	+	Entry[c]
	705-715	−	±	++	Entry
TM	716-746	+	ND	ND	

[a] For HCVpp infectivity data, +++, >90%; ++, between 30% and 90%; +, between 10% and 30%; ±, between 5% and 10%; −, <5%.
[b] ND, not defined. For HCVcc infectivity data, ++, <1 log lower than the wt; +, >1 log lower than the wt; ±, >2 logs lower than the wt; −, >3 logs lower than the wt. For HCVcc secretion data, ++, between 50% and 80%; +, between 20% and 50%; ±, between 10% and 20%; −, <10%.
[c] Suggested function based on our structural data.

despite a normal level of incorporation into HCVpp suggests a defect in virus entry.

Intradomain interactions within DI are crucial for E2 functions. Our data showed that the lack of infectivity of the DIb chimera is likely due to protein misfolding as shown in the CD81 pull-down (Fig. 1E). Since this construct contains only half of the predicted DI domain (34), we speculated that there might be an intradomain incompatibility between these two genotypes as reflected by the alteration of the CD81 binding region of the DI domain. We therefore made a new chimera containing DIa and DIb of genotype 1a in the context of E1E2 of genotype 2a to test this hypothesis. As shown in Fig. 3A, this chimera restored HCVpp infectivity by more than 50%. Furthermore, an increase in incorporation of E1E2 into HCVpp was observed, as was a better recognition of the intracellular form of E2 by CD81 (Fig. 3B).

Together, these data indicate that the two parts of the DI domain interact to form the CD81 binding region, which is in agreement with the recently proposed E2 model (34).

Role of the identified E2 regions in HCVcc assembly and infectivity. The HCVpp system is a well-established system to study the functions of HCV envelope glycoproteins. However, this system does not totally reflect the functions of HCV envelope proteins, since HCVpp is not assembled in the same compartment as HCVcc. Indeed, HCVcc assembles in an ER-derived compartment (49), whereas HCVpp is assembled in a post-Golgi compartment (64). Therefore, HCV envelope glycoproteins incorporated into HCVpp travel through the secretory pathway independently of the other viral components, whereas they are supposed to travel through the secretory pathway in association with nascent viral particles in the context of the HCVcc system. This can lead to differences in glycan maturation as well as in protein-protein interactions during assembly (70). We therefore analyzed some of our chimeric E2 proteins in the context of the HCVcc system.

We used the JFH-1 isolate containing the A4 epitope and the luciferase reporter gene in which we introduced separately the above-identified determinants of intergenotypic incompatibility. To further narrow down the determinants, we excluded some of the conserved fragments present in the HCVpp constructs. Moreover, we did not investigate the role of the 522-541 segment in the context of the HCVcc system, since we already showed (see above) that it is involved in intradomain interactions. However, we made an additional construct with the 682-704 segment, which induced a higher level of infectivity in the context of the HCVpp system. As controls, we used the wild-type JFH-1 isolate, a JFH-1 virus containing no envelope proteins (ΔE1E2), and the replication-defective mutant (GND) (71). None of the mutations affected genomic replication as analyzed by measuring luciferase activity at different times postelectroporation (data not shown). As shown in Fig. 4, chimeras 471-482 (HVR2) and 570-578 (IgVR) were noninfectious, and this lack of infectivity correlated with a defect in particle secretion as measured by a core release assay. Furthermore, we did not detect any intracellular infectivity for these two chimeras, indicating that the lack of infectivity of these mutants is not due to a defect in infectious particle secretion. It is worth noting that the lengths of HVR2 and IgVR differ by two amino acids between genotypes 1a and 2a. To determine whether the defect was not due to a change in the segment length, we extended HVR2 and IgVR of genotype 1a by inserting two corresponding amino acids from the 2a genotype or two alanine residues in the nonfunctional JFH-1 chimeras. However, none of the insertions was able to restore the infectivity of the chimeras (data not shown). This suggests that, instead of the length, it is the amino acid composition of the mutant viruses that affects E2 functions. Chimera 453-467 (within DII) was still infectious, but its extra- and intracellular infectivities were strongly reduced and this reduced infectivity also correlated with a low level of particle secretion (Fig. 4). Altogether, these data confirm some of the results obtained with the HCVpp system and they indicate that the 453-467

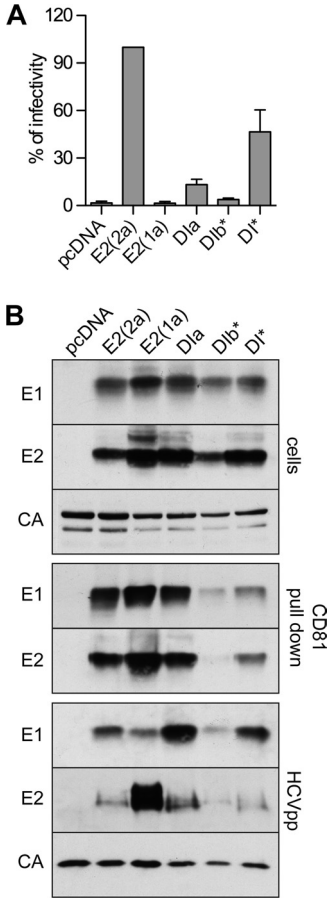

FIG. 3. Intergenotypic incompatibilities within CD81 binding domain DI. Wild-type 2a HCVpp [E2(2a)] and a noninfectious chimera [E2(1a)] were used as controls in the study. Chimeric constructs contained aa 384 to 444, corresponding to DIa and the nonconserved segment 522-541 within the second part of DI (labeled DIb*). Chimera DI* contained both regions. (A) Infectivity of chimeric particles assessed with the activity of reporter luciferase gene in infected Huh-7 cells. Results are presented as the percentage of infectivity in comparison to wild-type HCVpp [E2(2a)]. (B) 293T cells producing HCVpp were lysed and analyzed by Western blotting. HCVpp were pelleted from the supernatants on a 20% sucrose cushion and analyzed by Western blotting. E1E2 interaction with CD81 was verified by pull-down assay with CD81LEL fused to glutathione *S*-transferase. E1, E2, and capsid were detected using MAbs A4, 3/11, and R187, respectively.

region, HVR2, and IgVR of genotype 1a affect HCV infectivity by inducing a defect in particle assembly when introduced in the context of genotype 2a.

Chimeras with swapped segments within the ST region revealed some differences between the HCVpp and HCVcc systems. Chimera 667-681 was noninfectious in the HCVpp system (more precisely, segment 651-681 in Fig. 2B), whereas it showed less than 1 $\log_{10}$ decrease in infectivity in the HCVcc system (Fig. 4A). However, we cannot exclude the possibility that this difference is due to the Q-to-E change at position 661 (Fig. 1A), which is present in HCVpp chimera 651-681 but not in HCVcc chimera 667-681. Furthermore, chimera 682-704 was more infectious than the wild type in the HCVpp system (Fig. 2B), whereas its infectivity was reduced by 1 $\log_{10}$ in the HCVcc system (Fig. 4A). Core secretion of these chimeric viruses was lower than for the wild-type virus (Fig. 4B), and this likely contributes to their lower infectivity. Interestingly, the infectivity of chimera 705-715 was reduced by almost 3 $\log_{10}$ (Fig. 4A); however, this defect in infectivity was not due to a lack of particle secretion, since the level of secretion of core was close to that of the wild type (Fig. 4B). Importantly, the latter results correlate with those obtained with the HCVpp system and indicate that segment 705-715 plays a major role in HCV entry.

Characterization of the stem region determinant involved in the HCV entry process. Although the recently published E2 model provides some structural information for most of the regions identified in this work, the putative structure of the ST region remains limited to the identification of a highly conserved heptad repeat sequence necessary for heterodimerization with E1 (15, 59). Therefore, to better understand the role of the stem region, the structure and properties of this region were investigated. We first used bioinformatic tools to analyze this region. The degree of conservation among different genotypes was investigated. The amino acid repertoire derived from the alignment (Fig. 5A, panel b) revealed that amino acids are strictly conserved in 40% of the sequence positions (denoted by asterisks in Fig. 5A, panel a). In addition, the apparent variability is limited at most other positions, as indicated by both the similarity pattern (colons and dots) and the hydropathic pattern (Fig. 5A, panel c), where o, i, and n denote hydrophobic, hydrophilic, and neutral residues, respectively (see the legend to Fig. 5 for details). The conservation of the physicochemical properties at most positions indicates that the overall structure is certainly conserved among the different HCV genotypes. This is supported by secondary structure analyses that always predicted the presence of structured elements (α helix and/or β strand) for the same segments in the various genotypes as illustrated in Fig. 5A, panel d, for HCV clones H77 and JFH1 of genotypes 1a and 2a, respectively. Similar prediction patterns were observed for the other HCV genotypes (data not shown).

An examination of the hydrophobic plots in the E2 stem region indicates the presence of hydrophobic clusters, suggesting some potential binding to lipids. As illustrated in Fig. 5A, panel d, for E2 from HCV strain H77 and JFH1, the interfacial hydrophobicity plots calculated for sequences of various genotypes indicated that the segment of aa 663 to 703 or so, as well as segment 708-715, exhibits clear propensities to partition into the interface of a phospholipid bilayer (sequences highlighted in gray in Fig. 5A, panel d). To gain insight into the structure and lipotropic properties of the E2 aa 680-715 segment, the corresponding peptide of the JFH-1 strain (highlighted in bold in Fig. 5A, panel d; segment 684-719), designated E2-SC, was chemically synthesized, purified, and analyzed by CD and NMR. Note that the residues of this peptide were numbered according to the numbering of HCV reference strain H77, as recommended (35).

Conformation analyses of the E2-SC synthetic peptide by circular dichroism. Peptide E2-SC was soluble in water and gave a typical spectrum with a large negative band around 200 nm and a shoulder at 220 nm (Fig. 5B), indicating a mixture of random coil structures (~70%) with some poorly defined and/or residual secondary structures. The secondary structure of E2-SC was also examined in the presence of either lyso-

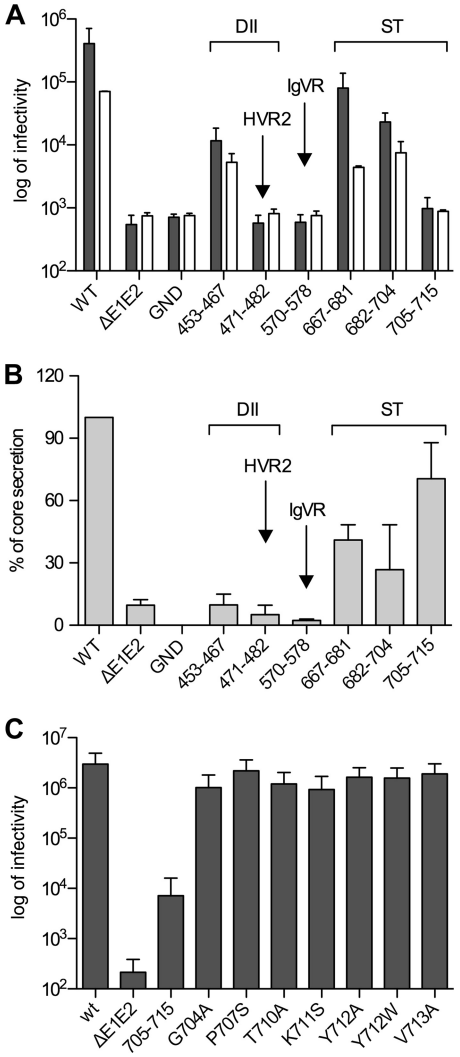

FIG. 4. Analysis of chimeric viruses produced in the HCVcc system. Wild type 2a virus (JFH-1) was used as a positive control. Viral RNA containing a deletion in the sequence encoding HCV envelope glycoproteins (ΔE1E2) and nonreplicative mutant containing a mutation in the polymerase sequence (GND) were used as negative controls. Chimeric viruses used in the study contained regions exchanged in DII (aa 453-467 and 471-482, corresponding to HVR2), aa 570-578, corresponding to IgVR, and aa 667-681, 682-704, and 705-715 within ST. (A) Extra- and intracellular infectivity of chimeric viruses. Viral RNA was electroporated into the Huh-7 cells. After 72 h, cells were lysed, and cleared supernatants were used to infect Huh-7 cells (intracellular infectivity is shown with white bars). Supernatants containing secreted virus were used to infect naïve Huh-7 cells (extracellular infectivity is shown with gray bars). Infectivity was assessed with the activity of the luciferase reporter gene in infected Huh-7 cells. The results are presented as the logarithm of infectivity. Note that in our JFH1 constructs, the N terminus of E1 has been modified to reconstruct the A4 epitope present in E1 of genotype 1a. (B) Secretion of chimeric viruses from electroporated cells. Supernatants collected from the electroporated cells were used to perform a core secretion assay. The presence of core in the samples is presented as the percentage of the core amount in comparison to wild-type JFH-1 virus. (C) Infectivity of HCVcc containing point mutations within aa 705-715 in the stem region. Wild-type 2a virus (JFH-1) was used as a positive control. Viral RNA containing a deletion in the sequence encoding HCV envelope glycoproteins (ΔE1E2) was used as a negative control. Chimera 705-715 was used to compare its infectivity with the infectivity of mutant viruses containing single amino acid changes. Viral RNA was electroporated into Huh-7 cells. After 72 h, the supernatants were collected and used to infect Huh-7 cells. Cells were lysed after 48 h, and the infectivity level was assessed by the activity of the luciferase reporter gene. The results are presented as the logarithm of the infectivity level.

phosphatidyl choline (LPC) or various detergents (SDS, *N*-dodecyl-β-D-maltoside [DM], dodecyl phosphocholine [DPC]) or cosolvents (TFE-water mixture) that mimic the membrane environment (Fig. 5B). These membrane mimetics were selected to reflect the various conditions in a true membrane, in order to gain a more comprehensive picture of the peptide conformational preferences. In the presence of the various detergents, CD spectra of the peptide exhibit the typical spectrum of α-helical folding, with a maximum at 190 nm and two minima, at 208 and 222 nm. The various CD deconvolution methods used indeed indicate predominant α-helix content (~40%), whatever the detergent used. The potential conformational preferences of E2-SC peptide were also probed in the presence of TFE, which is known to stabilize the folding of peptidic sequences, especially those exhibiting an intrinsic propensity to adopt an α-helical structure (3, 50). The peptide folding titration with increasing proportions of TFE gave spectra that were characteristic of α-helical folding, as illustrated in Fig. 5B (TFE 50%). Maximal amplitude was reached at 40% TFE and corresponds to an α-helical content of ~65% as measured. An isodichroic point was observed at 204 nm (data not shown), indicating that the peptide undergoes a simple transition from random coil to α helix, and according to the two-state model, equilibrium exists between the two conformers. This equilibrium together with the high α-helix content compared to that observed with detergents are consistent with an improved stabilization of the helical region in TFE, which is generally observed with these media. In summary, CD spectral analyses indicated the high propensity of E2-SC to interact with lipids and to adopt an α-helical structure upon lipid binding.

The E2-SC segment comprises an amphipathic α helix. Deuterated micellar SDS and DPC are popular membrane mimetic media for structure analyses of membrane peptides by liquid NMR (55). Unfortunately, samples of E2-SC peptide prepared in SDS and DPC displayed broad, poorly resolved NMR spectra. Nevertheless, an almost complete amino acid sequential attribution and ^{1}Hα chemical shift variation analysis were possible from spectra recorded with SDS, as were the identification of many sequential and medium-range NOE connectivities, as illustrated in Fig. 6A. However, this limited set of data did not permit the accurate modeling of the E2-SC peptide structure. We thus studied the three-dimensional structure of E2-SC dissolved in 50% TFE-d_2, which yielded well-resolved NMR spectra (data not shown). Sequential attribution of all spin systems was complete, and an overview of the sequential and medium-range NOE connectivities is shown in Fig. 6B. The NOE connectivity patterns demonstrate that the central part of the peptide, including residues 687 to 703, displays most characteristics of an α helix, including strong dNN(i, i + 1) and medium dαN(i, i + 1) sequential connectivities as well as weak dαN(i, i + 2), medium or strong dαN(i, i + 3) and dαβ(i, i + 3), and weak dαN(i, i + 4) medium-range

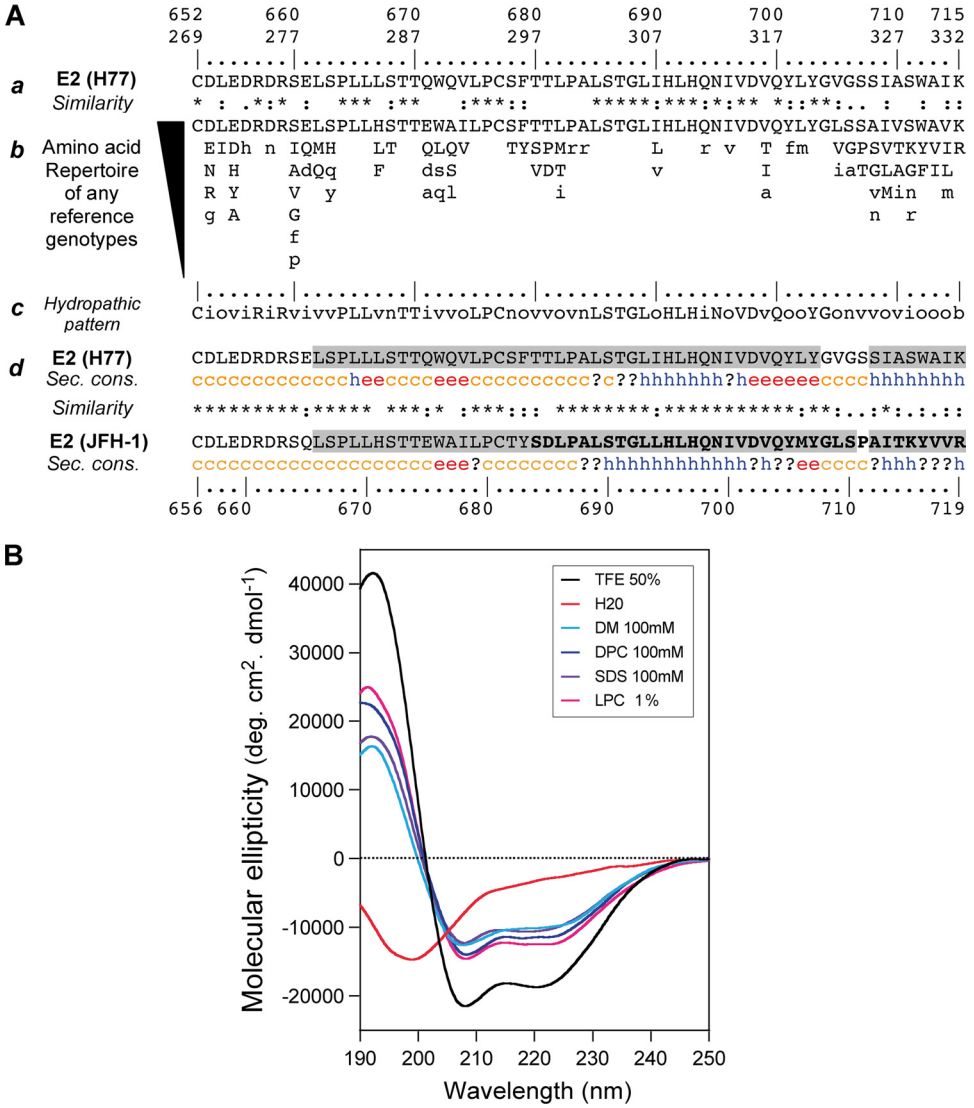

FIG. 5. Sequence analyses, predictions of secondary-structure, and membrane binding properties of the glycoprotein E2 stem region. (A) Amino acid repertoires. Amino acids are numbered with respect to the HCV polyprotein and E2 protein (top row) of the HCV H77 infectious clone (GenBank accession number AF009606). The amino acid repertoire of the 27 representative E2 sequences from confirmed HCV genotypes and subtypes (listed with accession numbers in Table 1 in reference 67), including the recently described genotype 7a (accession number EF108306; see the European HCV database for details [http://euhcvdb.ibcp.fr/; 10]), is given in panel b. The degree of amino acid conservation at each position can be inferred from the extent of variability (with the observed amino acids listed in decreasing order of frequency from top to bottom) together with the similarity index (a) according to the CLUSTAL W convention (asterisk, invariant; colon, highly similar; dot, similar) (69). Amino acids observed only one time at a given position among the 27 sequences are indicated by lowercase letters. (c) The physicochemical conservation of residues at each position is outlined by the consensus hydropathic pattern deduced from the consensus amino acid repertoire: o, hydrophobic position (F, I, W, Y, L, V, M, P, and C); n, neutral position (G, A, T, and S); i, hydrophilic position (K, Q, N, H, E, D, and R); v, variable position (i.e., when both hydrophobic and hydrophilic residues are observed at a given position). Fully conserved residues in any genotype are indicated by their one-letter code. (d) Consensus secondary-structure predictions of E2 from H77, and JFH1 clones (genotypes 1a and 2a, GenBank accession numbers AF009606 and AB047639, respectively), are indicated as helical (h, blue), extended (e, red), turn (t, green), or undetermined (coil [c], yellow). Predictions were made by using the Web-based algorithms DSC, HNNC, MLRC, PHD, Predator, SOPM, and SIMPA96 available at the NPSA website (http://npsa-pbil.ibcp.fr; reference 9 and the references therein). Amino acid sequence segments predicted to exhibit a propensity to partition into the interface of a phospholipid membrane are shaded in gray. Interfacial hydrophobicity plots were calculated with MPEx (http://blanco.biomol.uci.edu/mpex/) using the Wimley and White scale of interfacial hydrophobicity (74) and a window of 19 residues. The sequence comprising E2 aa 684 to 719 from the HCV JFH-1 infectious clone, which was used to prepare the peptide E2-SC described in this study, is indicated in bold. (B) Far-UV circular dichroism (CD) analyses of synthetic peptide E2-SC in various environments. CD spectra were recorded in water (H2O), complemented with either 50% 2,2,2-trifluoroethanol (TFE) or 1% L-α-lysophosphatidyl choline (LPC) or the following detergents: 100 mM sodium dodecyl sulfate (SDS), 100 mM *N*-dodecyl-β-D-maltoside (DM), or 100 mM dodecyl phosphocholine (DPC). sec. cons., secondary-structure consensus; deg., degree.

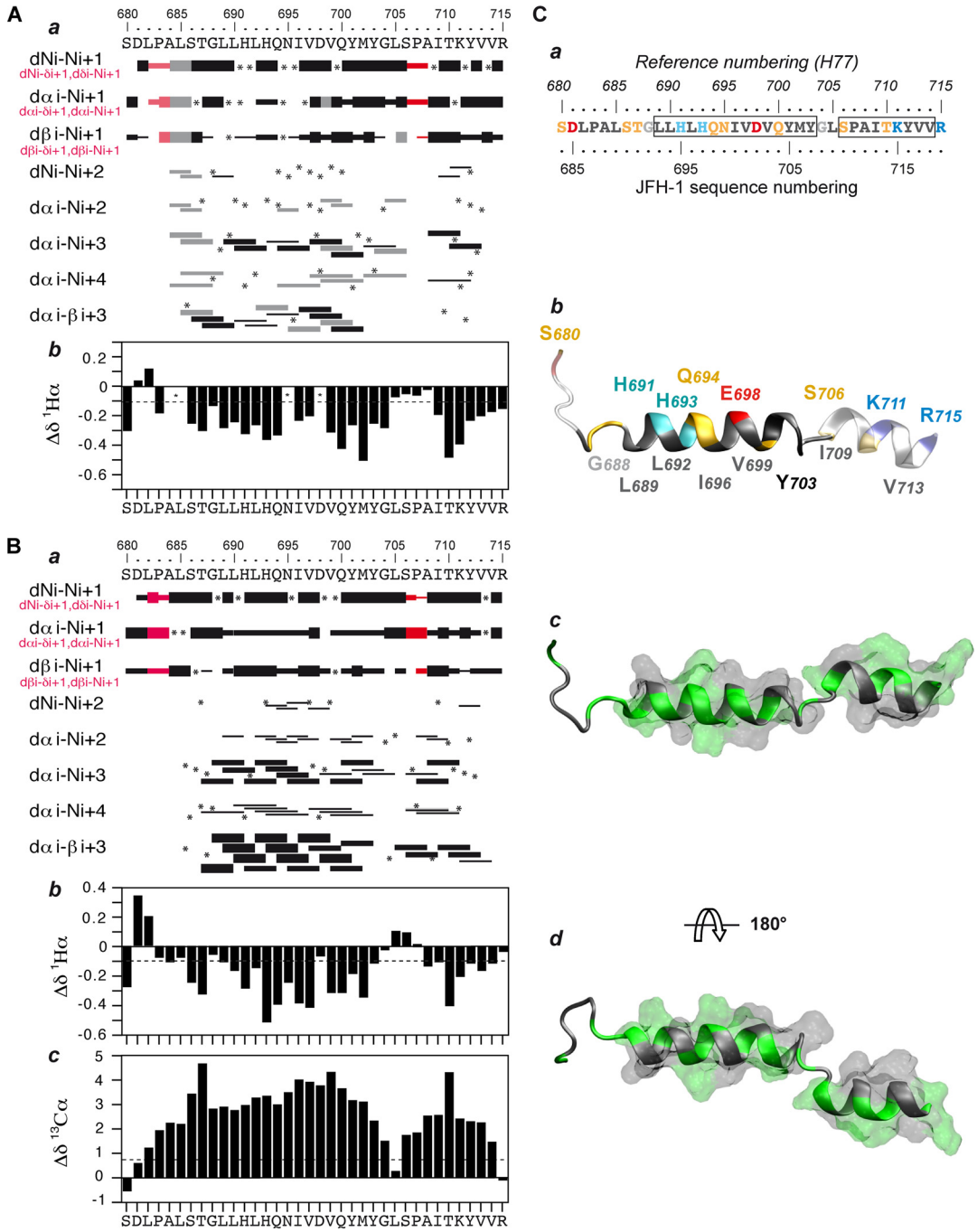

FIG. 6. NMR analysis and structure calculation of the E2-SC peptide. (A) Summary of sequential ($i, i + 1$) and medium-range ($i, i + 2$ to $i, i + 4$) NOEs (panel a) and ^{1}Hα chemical shift differences (in parts per million) (b) in 100 mM SDS. (B) Summary of sequential ($i, i + 1$) and medium-range ($i, i + 2$ to $i, i + 4$) NOEs (panel a) and ^{1}Hα and ^{13}Cα chemical shift differences (b and c) in 50% TFE. Sequential NOEs allowing the assignment of proline residues are indicated in red. Asterisks indicate that the presence of a NOE cross peak was not confirmed because of overlapping resonances (a) or the lack of Hα assignment (b). Intensities of NOEs are indicated by the height of the bars. Bars in gray indicate the NOEs that could not be unambiguously defined because of the incomplete assignment of residues. NMR-derived ^{1}Hα and ^{13}Cα chemical shift differences were calculated by subtraction of the experimental values from the reported random coil conformation values in either SDS (65) or TFE (48), respectively. The dashed lines indicate the standard threshold value of ΔHα (−0.1 ppm) or ΔCα (0.7 ppm [c]) for an α helix. (C). Amino acid sequence and NMR representative structure of E2-SC. (a) Sequence numbering refers to the H77 strain for reference numbering (35) and JFH-1 sequence numbering. Boxes indicate the α-helical segments. Residues are color-coded according to their physicochemical properties. Hydrophobic residues (A, V, L, F, M, I, W, and Y) are dark gray, and glycine residues are light gray. Polar residues (S, N, Q, and T) are yellow, and positively and negatively charged groups of basic (K, R) and acidic (E) residues are blue and red, respectively. Histidine residues are cyan. (b to d) Representative structure model of E2-SC showing the amphipathic character of α-helix 688-702 (aa 694 to 706 in the JFH-1 strain). (b) Side view with backbone residues (ribbon representation) colored as in panel a. (c and d) Hydrophilic side and hydrophobic side views of backbone and surface of amphipathic α-helix 688-702. Hydrophobic and hydrophilic residues are colored gray and green, respectively. Figures were generated from structure coordinates (PDB entry 2KZQ) using VMD (http://www.ks.uiuc.edu /Research/vmd/; [30]) and rendered with POV-Ray (http://www.povray.org).

TABLE 2. Statistics of final simulated annealing structures of the E2-SC peptide

Parameter	Value ± SD
Constraints used	
No. of distance restraints	
Intraresidue	0
Sequential	129
Medium range	87
Total	216
Statistics for the final X-PLOR structures	
No. of structures in the final set	36
X-PLOR energy (kcal · mol^{-1})	−91.9 ± 13.2
NOE violations	
No. > 0.5 Å	None
RMSD (Å)	0.081 ± 0.007
Deviation from idealized covalent geometry	
Angles (°)	0.54 ± 0.01
Impropers (°)	0.345 ± 0.008
Bonds (Å)	0.0037 ± 0.0001
RMSD (Å)	
Backbone (C′, Cα, N)	
Helix segment 689-700	0.44 ± 0.13
All residues	5.45 ± 1.34
All heavy atoms	
Helix segment 689-700	1.14 ± 0.19
All residues	6.78 ± 1.40
Ramachandran data (for 1,080 residues)[a]	
Residues in most-favored regions (%)	71.4
Residues in allowed regions (%)	27.0
Residues in generously allowed regions (%)	1.6
Residues in disallowed regions (%)	0

[a] Ramachandran data are from PROCHECK (37).

connectivities. Apart from this central helix, typical connectivities of the α-helical fold but of weaker intensities are also present in the C terminus of the peptide (aa 706 to 712 or so), indicating the presence of a fraying helix. The NOE-based indications of α-helical conformation were supported by the deviation of the ^{1}Hα and ^{13}Cα chemical shifts from random coil values (75), as shown in Fig. 6B, panels b and c. The long series of negative variation of ^{1}Hα chemical shifts ($\Delta\delta^{1}$Hα, <-0.1 ppm) as well as the positive variation of ^{13}Cα chemical shifts ($\Delta\delta^{13}$Cα, >0.7 ppm) are indeed typical of α-helical conformation.

The comparison of NOE connectivities and variations of Δd^{1}Hα chemical shifts observed with 50% TFE and 100 mM SDS along the peptide sequence reveals that the same segments exhibit α-helical folding (Fig. 6A and B). Interestingly, the N terminus of the central helix seems to extend up to residue 684 in 100 mM SDS. However, the weaker NOE intensities indicate that both helices are flexible and/or lack stability in SDS compared to results observed for 50% TFE. This is consistent with the higher content of α helix as measured by CD in 50% TFE and corresponds to the well-known stabilization of α-helical folding in this medium (3).

Based on the NOE-derived interproton distance constraints obtained with 50% TFE, a set of 50 structures was calculated with X-PLOR, and a final set of 36 low-energy structures that fully satisfied the experimental NMR data was retained. The number and types of NOE constraints used for the structure calculations as well as the statistics for this final set of 36 structures are given in Table 2. Superimposition of the 36 structures (Fig. 7) shows two quite well defined helices connected by a small flexible segment around Gly 704, due to presence of a proline residue in position $i + 3$ (Pro 707). The main part of the central helix (residues 689-700) is well de-

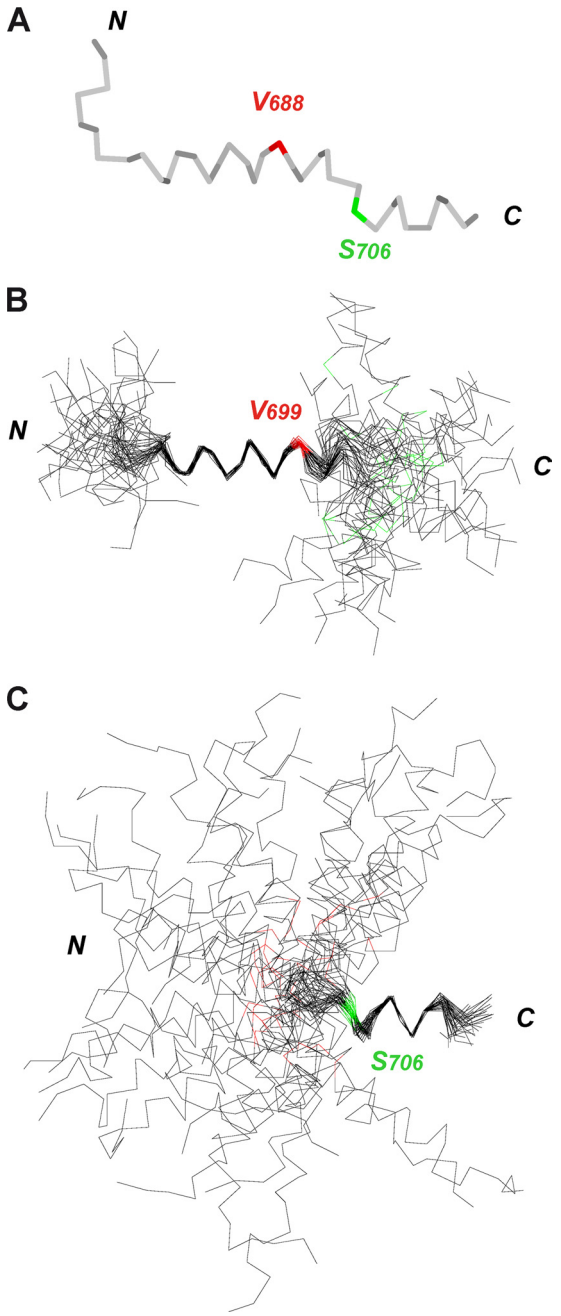

FIG. 7. Structural characterization of the E2-SC peptide in TFE 50%. (A) Representative structure model. (B and C) Superimposition of the backbone heavy atoms (N, Cα, and C′) of the 36 final structures (PDB entry 2KZQ) for the best overlap of residues 688-699 and 709-712, respectively, which correspond to canonical α-helical residues.

fined, with a backbone RMSD of 0.44 Å (Table 2). This helix extended also on some structures up to residue 703. The C-terminal helix is less well defined and behaves as a fraying helix, including residues 706 to 714 or so. The apparent instability of this helix in the E2-SC peptide context is likely due to the lack of the downstream sequence corresponding to the predicted transmembrane helical domain of E2.

As illustrated in Fig. 6C, the asymmetric distribution of polar and hydrophobic residues on each side of the central helix clearly reveals the mainly amphipathic character of this α helix. The hydrophobic residues, including two tyrosine residues, are quite well positioned within or on the edges of the hydrophobic side, suggesting their essential role in a putative interaction with the membrane interface. Indeed, tyrosines are frequently found at the membrane interface (26). These structural features, together with the clear propensity of the E2-SC peptide to adopt an α-helical structure upon binding to lipid-like molecules, suggest that the central amphipathic α helix associates with the membrane interface, at least transiently, in an in-plane topology. The C-terminal helix also appeared to be relatively amphiphilic, with a hydrophobic face formed by amino acids 709-710 and 712-714 and a hydrophilic side of amino acids 711 and 715. Although variability between genotypes 2a and 1a was observed, the conformational properties of this region are conserved. The amphiphilicity of this helix together with the presence of aromatic residues and its location upstream of the TM domain of E2 suggest that it is located at the membrane interface, maybe in an in-plane topology.

The structural data obtained for E2-SC provided us with a framework for additional mutations in the 705-715 region identified in our biological experiments. To further characterize the role of segment 705-715 in HCV entry, we therefore introduced point mutations in this region in the context of the HCVcc system. Based on sequence comparison between genotypes 1a and 2a, we designed a panel of mutants: G704A, P707S, T710A, K711S, Y712A, Y712W, and V713A. Alanine substitutions were introduced to identify the potential role of specific amino acids, whereas the other substitutions were based on the differences between 2a and 1a genotypes. Although a slight decrease in HCVcc infectivity was observed for the G704A, T710A, and K711S mutants, none of the individual mutations can explain the defect in infectivity of chimera 705-715 (Fig. 4C). As these single mutations are not supposed to affect the α-helix structure, these data suggest that several residues within segment 705-715 cooperate to play a role in HCV entry, maybe thanks to multiple binding points with an interacting partner.

DISCUSSION

Viral envelope glycoproteins play an important role at different steps of the viral life cycle. During virion morphogenesis, they take part in the assembly process, whereas in the early steps of the viral life cycle, they are involved in receptor binding and in fusion between the viral envelope and a cellular membrane. To fulfill these functions, viral envelope glycoproteins have to adopt dramatically different conformations at these different steps of the infectious cycle. Importantly, these conformational changes have to occur at a precise time and thus have to be tightly controlled. Despite extensive research on HCV envelope glycoproteins, the structures and functions of these proteins remain poorly understood. Here, we used a genetic approach to identify functional determinants in HCV glycoprotein E2. By generating HCVpp containing E1 and E2 from different genotypes, we identified intergenotypic incompatibilities between these two proteins. By using a nonfunctional E1E2 complex, we identified new functional regions in E2 by exchanging protein regions between two incompatible genotypes. This led to the identification of several determinants of the E2 ectodomain that play a role in E1E2 assembly (Table 1). Furthermore, we also characterized the structural and lipid binding features of the C-terminal part of the ST segment by CD and NMR using a synthetic peptide denoted E2-SC. This segment, which is involved in HCV entry and located close to the TM domain, includes a central amphipathic helix, which folds upon binding to lipid mimetics. Its features suggest that this helix could easily switch from helical to random conformation, depending on its microenvironment and/or binding partners. Together, these data highlight new functional regions in HCV envelope glycoprotein E2.

Intergenotypic incompatibilities exist between HCV glycoproteins E1 and E2 from different genotypes. Although the overall structure of HCV proteins is not expected to differ significantly between HCV genotypes, coevolution within a genotype or subtype can potentially lead to functional incompatibilities between partner proteins. Such genetic incompatibilities have indeed already been reported for HCV, highlighting potential protein-protein interactions between viral polypeptides (2, 77). In the case of HCV envelope glycoproteins, biochemical analyses have shown that they assemble in the cell as noncovalent heterodimers (11). Furthermore, these interactions are important for the cooperative folding of these two proteins (reviewed in reference 38). It is therefore not surprising that HCV envelope glycoproteins have coevolved in the different genotypes and that this coevolution can lead to functional intergenotypic incompatibilities between E1 and E2. It is however more puzzling that in the case of genotype 1a, E1 was compatible with the E2 of any genotype tested. A potential explanation for this phenotype is that the E1 protein of genotype 1a has more flexibility to accommodate changes in conformation or oligomerization during the fusion process. However, this needs further investigation.

Residues of the ST region close to the TM domain play a major role in HCV entry. Indeed, HCVcc infectivity was reduced by almost 3 logs when segment 705-715 of genotype 1a was introduced in the context of E1E2 of genotype 2a. We have previously shown that the interactions between TM domains play a major role in E1E2 heterodimerization (8) as well as in virus entry (5, 6). Since segment 705-715 corresponds to the upstream sequence of the E2 transmembrane domain, these two regions might be functionally connected for the assembly of the E1E2 heterodimer. However, heterodimerization was not affected for the 705-715 chimera, as shown by coprecipitation in a CD81 pull-down assay. Furthermore, particle assembly and release was not affected by this mutation. The incompatibility between genotypes 1a and 2a in the ST region therefore highlights a role for the 705-715 segment in the entry process. The ST region is relatively flexible and is supposed to play a major role in the reorganization of the envelope glycoproteins during the fusion process (34). Amino acid residues

705 to 715 are therefore likely involved in interactions with E1 region at some stage of the fusion process.

The aa sequence analyses and the structural investigations of the corresponding synthetic peptide E2-SC by CD in various media clearly show that this region exhibits potential lipid binding properties and could fold into α helices upon binding. The three-dimensional structure analysis of this peptide in SDS or 50% TFE used to probe the peptide conformational preferences as well as to mimic the membrane environment revealed that the major structural elements consist of a central amphipathic helix (689 to 703, but it could extend to aa 684 as revealed by SDS analysis) and a C-terminal fraying helix (706 to 714 or so) connected by a short flexible segment, including a glycine residue (704). Both helices require a hydrophobic environment for folding, indicating that lipid interactions and/or protein interactions could contribute to their structural stability. In addition, the fraying of the C-terminal helix could be due to the absence of the downstream transmembrane sequence, which would likely stabilize this helix. Its relative amphiphilicity and its connection with the TM of E2 suggest that this helix should be located at the membrane interface, maybe with an in-plane topology. The amphipathic nature of the highly conserved central helix 689-703 together with the helix folding upon binding to lipid mimetics suggest that this helix could bind in-plane to a membrane interface. However, the relatively low free energy of membrane association, as calculated using the MPEX program (74), suggests that this helix could be easily released from the membrane interface. This is consistent with the limited stability of this amphipathic helix in SDS. One can thus hypothesize that this helix is able to ensure a conformational transition between helix folding when bound to the membrane interface and a coil state upon membrane release. According to the conformational change of the stem region proposed in the model of fusion events for class II glycoproteins (22, 23), it is tempting to speculate that this amphipathic helix could ultimately fold again upon binding to the trimeric postfusion complex of glycoproteins.

HVR2 and IgVR are essential determinants for HCV particle assembly. Based on results with HVR1 mutants, it was thought that the most variable regions on of E2 would be dispensable for HCV infectivity. Indeed, although it reduces infectivity, the deletion of HVR1 in the context of an infectious virus is not lethal (21). Furthermore, deletion of the three variable regions HVR1, HVR2, and IgVR in a truncated form of E2 does not seem to affect its folding as measured by binding of conformation-dependent MAbs and CD81 pull-down (44). However, very recent data indicate that deletion of HVR2 or IgVR is lethal in the HCVcc system, suggesting that the presence of these regions in E2 can play a functional role in virus assembly (45). In our case, we used a less drastic approach consisting of replacing these regions with the corresponding segment from another genotype. In such chimeric viruses, introducing HVR2 or IgVR from genotype 1a in the context of an infectious clone of genotype 2a was also lethal for the production of infectious virus, which was due to an alteration in the production of viral particles as measured by a core release assay.

Exchanging HVR2 or IgVR affects the incorporation of E1 into HCVpp. In the context of the HCVpp system, the recognition of the chimeric E2 by CD81 suggests that at least domain DI of this protein is properly folded after replacing HVR2 or IgVR by the corresponding region from another genotype. However, the level of incorporation of the E1 into HCVpp was barely detectable for these chimeras. This lack of E1 incorporation into HCVpp is in contrast with the interactions between E1 and E2 as observed in the CD81 pull-down assay. However, further analyses of the intracellular E1E2 complexes recognized by CD81 indicated that E1 formed disulfide bond-linked high-molecular-weight complexes with these chimeric E2 proteins (data not shown). Interestingly, we have recently shown that in the context of the HCVcc system, virion-associated E1 and E2 envelope glycoproteins form large covalent complexes stabilized by disulfide bridges, whereas the intracellular forms of these proteins assemble as noncovalent heterodimers (70). The presence of disulfide bridges between HCV envelope glycoproteins suggests that lateral protein-protein interactions assisted by disulfide-bond formation might play an active role in the budding process of HCV particles. Therefore, we cannot exclude the possibility that in the context of our chimeric viruses, the introduction of HVR2 or IgVR from another genotype leads to the formation of premature intermolecular disulfide bonds within infected cells, which is no longer coordinated with the other steps of the assembly process. It is worth noting that, when the whole ectodomain of E2 was replaced by the corresponding sequence from genotype 1a, E1 was correctly incorporated into HCVpp, suggesting that chimeras containing HVR2 or IgVR induce an additional defect, which is likely due to interdomain incompatibilities within E2. There might indeed be molecular cross-talk between HVR2 or IgVR and domain DIII and/or the ST region, since a defect in assembly was also observed when we dissociated the DI-DII region from the DIII-TM region (Fig. 1).

In addition to interdomain incompatibilities within E2, we also identified a genetic incompatibility within a single E2 domain. Indeed, exchanging sequences between genotypes 1a and 2a within domain DI can lead to protein misfolding. as shown by replacing DIb of genotype 2a with the equivalent sequence from genotype 1a, which led to the absence of recognition of E2 by CD81. Importantly, infectivity and CD81 binding were restored when both DIa and DIb of genotype 1a were introduced in the context of E1E2 of genotype 2a. Therefore, our data indicate that the two parts of the DI domain interact together to form the major CD81 binding determinant, which is in agreement with the recently proposed E2 model (34). It is worth noting that the chimeric E2 protein containing DI domain from genotype 1a was still less efficiently pulled down by CD81, suggesting that in addition to the major CD81 determinants identified in DI (13, 56), other residues within DIII might also modulate CD81 binding, as suggested previously (34, 62). However, we cannot exclude the possibility that the involvement of domain DIII is indirect since mutations in this domain, which affect CD81 binding, can affect DIII folding (31).

In this study, we cannot exclude the possibility of some effect of the changes introduced in E1 in reconstructing the A4 epitope. Indeed, we observed some decrease in HCVpp infectivity when the A4 epitope was engineered with E1 of genotype 2a, suggesting some modulation of E1E2 interaction mediated by this region. However, JFH1 infectivity was very similar in the presence or absence of the modified epitope, suggesting

that the change in the A4 epitope has only minor effects in the HCVcc system.

In conclusion, we identified several important determinants of E2 ectodomain that are involved in virion assembly or in HCV entry. We also revealed the presence of a well conserved amphipathic helix in the stem region, which likely undergoes conformational changes during the fusion process. Together, these data highlight the complexity of the intermolecular interplay between E1 and E2.

ACKNOWLEDGMENTS

We are grateful to Czeslaw Wychowski, Nathalie Callens, François Helle, and Costin-Ioan Popescu for their scientific input. We thank Sumedha Roy and Bhavna Tandon for their technical assistance. We also thank Sophana Ung for advice on preparing the figures. We are also grateful to T. Wakita, F. L. Cosset, R. Bartenschlager, and J. McKeating for providing reagents. Peptide synthesis and CD experiments were performed with the platforms Centre Commun de Microanalyse des Proteines and Production et Analyze de Proteines from the IFR 128 BioSciences Gerland—Lyon Sud.

This work was supported by the French Agence Nationale de Recherche sur le sida et les hépatites virales (ANRS), a Marie Curie Research Training Network grant (MRTN-CT-2006-035599), and the European Commission through the EMBRACE project (LHSG-CT-2004-512092). A.A. was successively supported by a Marie Curie Research Training Network grant (MRTN-CT-2006-035599) and a fellowship from the ANRS. J.D. is an international scholar of the Howard Hughes Medical Institute.

REFERENCES

1. **Bartosch, B., J. Dubuisson, and F. L. Cosset.** 2003. Infectious hepatitis C virus pseudo-particles containing functional E1-E2 envelope protein complexes. J. Exp. Med. **197:**633–642.
2. **Brohm, C., et al.** 2009. Characterization of determinants important for hepatitis C virus p7 function in morphogenesis by using trans-complementation. J. Virol. **83:**11682–11693.
3. **Buck, M.** 1998. Trifluoroethanol and colleagues: cosolvents come of age: recent studies with peptides and proteins. Q. Rev. Biophys. **31:**297–355.
4. **Choo, Q. L., et al.** 1989. Isolation of a cDNA clone derived from a blood-borne non-A, non-B viral hepatitis genome. Science **244:**359–362.
5. **Ciczora, Y., et al.** 2005. Contribution of the charged residues of hepatitis C virus glycoprotein E2 transmembrane domain to the functions of the E1E2 heterodimer. J. Gen. Virol. **86:**2793–2798.
6. **Ciczora, Y., N. Callens, F. Penin, E. I. Pecheur, and J. Dubuisson.** 2007. Transmembrane domains of hepatitis C virus envelope glycoproteins: residues involved in E1E2 heterodimerization and involvement of these domains in virus entry. J. Virol. **81:**2372–2381.
7. **Cocquerel, L., C. C. Kuo, J. Dubuisson, and S. Levy.** 2003. CD81-dependent binding of hepatitis C virus E1E2 heterodimers. J. Virol. **77:**10677–10683.
8. **Cocquerel, L., et al.** 2002. Topological changes in the transmembrane domains of hepatitis C virus envelope glycoproteins. EMBO J. **21:**2893–2902.
9. **Combet, C., C. Blanchet, C. Geourjon, and G. Deleage.** 2000. NPS@: network protein sequence analysis. Trends Biochem. Sci. **25:**147–150.
10. **Combet, C., et al.** 2007. euHCVdb: the European hepatitis C virus database. Nucleic Acids Res. **35:**D363–D366.
11. **Deleersnyder, V., et al.** 1997. Formation of native hepatitis C virus glycoprotein complexes. J. Virol. **71:**697–704.
12. **Delgrange, D., et al.** 2007. Robust production of infectious viral particles in Huh-7 cells by introducing mutations in hepatitis C virus structural proteins. J. Gen. Virol. **88:**2495–2503.
13. **Drummer, H. E., I. Boo, A. L. Maerz, and P. Poumbourios.** 2006. A conserved Gly436-Trp-Leu-Ala-Gly-Leu-Phe-Tyr motif in hepatitis C virus glycoprotein E2 is a determinant of CD81 binding and viral entry. J. Virol. **80:**7844–7853.
14. **Drummer, H. E., A. Maerz, and P. Poumbourios.** 2003. Cell surface expression of functional hepatitis C virus E1 and E2 glycoproteins. FEBS Lett. **546:**385–390.
15. **Drummer, H. E., and P. Poumbourios.** 2004. Hepatitis C virus glycoprotein E2 contains a membrane-proximal heptad repeat sequence that is essential for E1E2 glycoprotein heterodimerization and viral entry. J. Biol. Chem. **279:**30066–30072.
16. **Dubuisson, J., et al.** 1994. Formation and intracellular localization of hepatitis C virus envelope glycoprotein complexes expressed by recombinant vaccinia and Sindbis viruses. J. Virol. **68:**6147–6160.
17. **Dubuisson, J., F. Penin, and D. Moradpour.** 2002. Interaction of hepatitis C virus proteins with host cell membranes and lipids. Trends Cell Biol. **12:**517–523.
18. **Favier, A., et al.** 2002. Solution structure and dynamics of Crh, the Bacillus subtilis catabolite repression HPr. J. Mol. Biol. **317:**131–144.
19. **Flint, M., et al.** 2000. Functional characterization of intracellular and secreted forms of a truncated hepatitis C virus E2 glycoprotein. J. Virol. **74:**702–709.
20. **Flint, M., et al.** 1999. Characterization of hepatitis C virus E2 glycoprotein interaction with a putative cellular receptor, CD81. J. Virol. **73:**6235–6244.
21. **Forns, X., et al.** 2000. Hepatitis C virus lacking the hypervariable region 1 of the second envelope protein is infectious and causes acute resolving or persistent infection in chimpanzees. Proc. Natl. Acad. Sci. U. S. A. **97:**13318–13323.
22. **Gibbons, D. L., et al.** 2003. Visualization of the target-membrane-inserted fusion protein of Semliki Forest virus by combined electron microscopy and crystallography. Cell **114:**573–583.
23. **Gibbons, D. L., et al.** 2004. Conformational change and protein-protein interactions of the fusion protein of Semliki Forest virus. Nature **427:**320–325.
24. **Gottwein, J. M., et al.** 2009. Development and characterization of hepatitis C virus genotype 1-7 cell culture systems: role of CD81 and scavenger receptor class B type I and effect of antiviral drugs. Hepatology **49:**364–377.
25. **Goueslain, L., et al.** 2010. Identification of GBF1 as a cellular factor required for hepatitis C virus RNA replication. J. Virol. **84:**773–787.
26. **Granseth, E., G. von Heijne, and A. Elofsson.** 2005. A study of the membrane-water interface region of membrane proteins. J. Mol. Biol. **346:**377–385.
27. **Haid, S., T. Pietschmann, and E. I. Pecheur.** 2009. Low pH-dependent hepatitis C virus membrane fusion depends on E2 integrity, target lipid composition, and density of virus particles. J. Biol. Chem. **284:**17657–17667.
28. **Helle, F., et al.** 2007. The neutralizing activity of anti-hepatitis C virus antibodies is modulated by specific glycans on the E2 envelope protein. J. Virol. **81:**8101–8111.
29. **Hsu, M., et al.** 2003. Hepatitis C virus glycoproteins mediate pH-dependent cell entry of pseudotyped retroviral particles. Proc. Natl. Acad. Sci. U. S. A. **100:**7271–7276.
30. **Humphrey, W., A. Dalke, and K. Schulten.** 1996. VMD: visual molecular dynamics. J. Mol. Graph. **14:**33–38, 27–28.
31. **Iacob, R. E., Z. Keck, O. Olson, S. K. Foung, and K. B. Tomer.** 2008. Structural elucidation of critical residues involved in binding of human monoclonal antibodies to hepatitis C virus E2 envelope glycoprotein. Biochim. Biophys. Acta **1784:**530–542.
32. **Kielian, M., and F. A. Rey.** 2006. Virus membrane-fusion proteins: more than one way to make a hairpin. Nat. Rev. Microbiol. **4:**67–76.
33. **Koradi, R., M. Billeter, and K. Wuthrich.** 1996. MOLMOL: a program for display and analysis of macromolecular structures. J. Mol. Graph. **14:**51–55, 29–32.
34. **Krey, T., et al.** 2010. The disulfide bonds in glycoprotein e2 of hepatitis C virus reveal the tertiary organization of the molecule. PLoS. Pathog. **6:**e1000762.
35. **Kuiken, C., et al.** 2006. A comprehensive system for consistent numbering of HCV sequences, proteins and epitopes. Hepatology **44:**1355–1361.
36. **Kuiken, C., and P. Simmonds.** 2009. Nomenclature and numbering of the hepatitis C virus. Methods Mol. Biol. **510:**33–53.
37. **Laskowski, R. A., M. W. MacArthur, D. S. Moss, and J. M. Thornton.** 1993. PROCHECK: a program to check the stereochemical quality of protein structures. J. Appl. Crystallogr. **26:**283–291.
38. **Lavie, M., A. Goffard, and J. Dubuisson.** 2007. Assembly of a functional HCV glycoprotein heterodimer. Curr. Issues Mol. Biol. **9:**71–86.
39. **Lavillette, D., et al.** 2006. Hepatitis C virus glycoproteins mediate low pH-dependent membrane fusion with liposomes. J. Biol. Chem. **281:**3909–3917.
40. **Lavillette, D., et al.** 2007. Characterization of fusion determinants points to the involvement of three discrete regions of both E1 and E2 glycoproteins in the membrane fusion process of hepatitis C virus. J. Virol. **81:**8752–8765.
41. **Lemon, S. M., C. Walker, M. J. Alter, and M. Yi.** 2007. Hepatitis virus, p. 1253–1304. *In* D. M. Knipe, et al. (ed.), Fields virology, 5th ed. Lippincott Williams & Wilkins, Philadelphia, PA.
42. **Lindenbach, B. D., et al.** 2005. Complete replication of hepatitis C virus in cell culture. Science **309:**623–626.
43. **Marcellin, P.** 2009. Hepatitis B and hepatitis C in 2009. Liver Int. **29**(Suppl. 1)**:**1–8.
44. **McCaffrey, K., I. Boo, P. Poumbourios, and H. E. Drummer.** 2007. Expression and characterization of a minimal hepatitis C virus glycoprotein E2 core domain that retains CD81 binding. J. Virol. **81:**9584–9590.
45. **McCaffrey, K., H. Gouklani, I. Boo, P. Poumbourios, and H. E. Drummer.** 2011. The variable regions of hepatitis C virus glycoprotein E2 have an essential structural role in glycoprotein assembly and virion infectivity. J. Gen. Virol. **92:**112–121.
46. **McKeating, J. A., et al.** 2004. Diverse hepatitis C virus glycoproteins mediate viral infection in a CD81-dependent manner. J. Virol. **78:**8496–8505.
47. **Mederacke, I., et al.** 2009. Performance and clinical utility of a novel fully automated quantitative HCV-core antigen assay. J. Clin. Virol. **46:**210–215.

48. **Merutka, G., H. J. Dyson, and P. E. Wright.** 1995. 'Random coil' 1H chemical shifts obtained as a function of temperature and trifluoroethanol concentration for the peptide series GGXGG. J. Biomol. NMR **5:**14–24.
49. **Miyanari, Y., et al.** 2007. The lipid droplet is an important organelle for hepatitis C virus production. Nat. Cell Biol. **9:**1089–1097.
50. **Montserret, R., et al.** 1999. Structural analysis of the heparin-binding site of the NC1 domain of collagen XIV by CD and NMR. Biochemistry **38:**6479–6488.
51. **Morota, K., et al.** 2009. A new sensitive and automated chemiluminescent microparticle immunoassay for quantitative determination of hepatitis C virus core antigen. J. Virol. Methods **157:**8–14.
52. **Nakabayashi, H., K. Taketa, K. Miyano, T. Yamane, and J. Sato.** 1982. Growth of human hepatoma cells lines with differentiated functions in chemically defined medium. Cancer Res. **42:**3858–3863.
53. **Op De Beeck, A., et al.** 2000. The transmembrane domains of hepatitis C virus envelope glycoproteins E1 and E2 play a major role in heterodimerization. J. Biol. Chem. **275:**31428–31437.
54. **Op De Beeck, A., et al.** 2004. Characterization of functional hepatitis C virus envelope glycoproteins. J. Virol. **78:**2994–3002.
55. **Opella, S. J.** 1997. NMR and membrane proteins. Nat. Struct. Biol. **4**(Suppl.)**:**845–848.
56. **Owsianka, A. M., et al.** 2006. Identification of conserved residues in the E2 envelope glycoprotein of the hepatitis C virus that are critical for CD81 binding. J. Virol. **80:**8695–8704.
57. **Penin, F., J. Dubuisson, F. A. Rey, D. Moradpour, and J. M. Pawlotsky.** 2004. Structural biology of hepatitis C virus. Hepatology **39:**5–19.
58. **Penin, F., et al.** 1997. Three-dimensional structure of the DNA-binding domain of the fructose repressor from Escherichia coli by 1H and 15N NMR. J. Mol. Biol. **270:**496–510.
59. **Perez-Berna, A. J., M. R. Moreno, J. Guillen, A. Bernabeu, and J. Villalain.** 2006. The membrane-active regions of the hepatitis C virus E1 and E2 envelope glycoproteins. Biochemistry **45:**3755–3768.
60. **Pileri, P., et al.** 1998. Binding of hepatitis C virus to CD81. Science **282:**938–941.
61. **Popescu, C. I., and J. Dubuisson.** 2010. Role of lipid metabolism in hepatitis C virus assembly and entry. Biol. Cell **102:**63–74.
62. **Rothwangl, K. B., B. Manicassamy, S. L. Uprichard, and L. Rong.** 2008. Dissecting the role of putative CD81 binding regions of E2 in mediating HCV entry: putative CD81 binding region 1 is not involved in CD81 binding. Virol. J. **5:**46.
63. **Russell, R. S., et al.** 2009. Mutational analysis of the hepatitis C virus E1 glycoprotein in retroviral pseudoparticles and cell-culture-derived H77/JFH1 chimeric infectious virus particles. J. Viral Hepat. **16:**621–632.
64. **Sandrin, V., et al.** 2005. Assembly of functional hepatitis C virus glycoproteins on infectious pseudoparticles occurs intracellularly and requires concomitant incorporation of E1 and E2 glycoproteins. J. Gen. Virol. **86:**3189–3199.
65. **Schwarzinger, S., et al.** 2001. Sequence-dependent correction of random coil NMR chemical shifts. J. Am. Chem. Soc. **123:**2970–2978.
66. **Schwieters, C. D., J. J. Kuszewski, N. Tjandra, and G. M. Clore.** 2003. The Xplor-NIH NMR molecular structure determination package. J. Magn. Reson. **160:**65–73.
67. **Simmonds, P., et al.** 2005. Consensus proposals for a unified system of nomenclature of hepatitis C virus genotypes. Hepatology **42:**962–973.
68. **Tarr, A. W., et al.** 2006. Characterization of the hepatitis C virus E2 epitope defined by the broadly neutralizing monoclonal antibody AP33. Hepatology **43:**592–601.
69. **Thompson, J. D., D. G. Higgins, and T. J. Gibson.** 1994. CLUSTAL W: improving the sensitivity of progressive multiple sequence alignment through sequence weighting, position-specific gap penalties and weight matrix choice. Nucleic Acids Res. **22:**4673–4680.
70. **Vieyres, G., et al.** 2010. Characterization of the envelope glycoproteins associated with infectious hepatitis C virus. J. Virol. **84:**10159–10168.
71. **Wakita, T., et al.** 2005. Production of infectious hepatitis C virus in tissue culture from a cloned viral genome. Nat. Med. **11:**791–796.
72. **Wasley, A., and M. J. Alter.** 2000. Epidemiology of hepatitis C: geographic differences and temporal trends. Semin. Liver Dis. **20:**1–16.
73. **Whitmore, L., and B. A. Wallace.** 2004. DICHROWEB, an online server for protein secondary structure analyses from circular dichroism spectroscopic data. Nucleic Acids Res. **32:**W668–W673.
74. **Wimley, W. C., and S. H. White.** 1996. Experimentally determined hydrophobicity scale for proteins at membrane interfaces. Nat. Struct. Biol. **3:**842–848.
75. **Wishart, D. S., B. D. Sykes, and F. M. Richards.** 1992. The chemical shift index: a fast and simple method for the assignment of protein secondary structure through NMR spectroscopy. Biochemistry **31:**1647–1651.
76. **Wuthrich, K.** 1986. NMR of proteins and nucleic acids. J. Wiley and Sons, New York, NY.
77. **Yi, M., Y. Ma, J. Yates, and S. M. Lemon.** 2007. Compensatory mutations in E1, p7, NS2, and NS3 enhance yields of cell culture-infectious intergenotypic chimeric hepatitis C virus. J. Virol. **81:**629–638.
78. **Zhong, J., et al.** 2005. Robust hepatitis C virus infection in vitro. Proc. Natl. Acad. Sci. U. S. A. **102:**9294–9299.